AFRL-RX-WP-TP-2012-0376

PROCESSING AND TESTING Re2Si207 MATRIX COMPOSITES (PREPRINT)

Randall S. Hay and Michael K. Cinibulk
Composites Branch
Structural Materials Division

Emmanuel E. Boakye, Kristin Keller, Pavel S. Mogilevsky, and T.A. Parthasarathy
UES, Inc.

M. Ahrens
Wright State University

JULY 2012
Interim

STINFO COPY

REPORT DOCUMENTATION PAGE

Form Approved
OMB No. 0704-0188

The public reporting burden for this collection of information is estimated to average 1 hour per response, including the time for reviewing instructions, searching existing data sources, searching existing data sources, gathering and maintaining the data needed, and completing and reviewing the collection of information. Send comments regarding this burden estimate or any other aspect of this collection of information, including suggestions for reducing this burden, to Department of Defense, Washington Headquarters Services, Directorate for Information Operations and Reports (0704-0188), 1215 Jefferson Davis Highway, Suite 1204, Arlington, VA 22202-4302. Respondents should be aware that notwithstanding any other provision of law, no person shall be subject to any penalty for failing to comply with a collection of information if it does not display a currently valid OMB control number. **PLEASE DO NOT RETURN YOUR FORM TO THE ABOVE ADDRESS.**

1. REPORT DATE *(DD-MM-YY)*	2. REPORT TYPE	3. DATES COVERED *(From - To)*
July 2012	Technical Paper	1 June 2012 – 1 July 2012

4. TITLE AND SUBTITLE
PROCESSING AND TESTING Re2Si207 MATRIX COMPOSITES (PREPRINT)

5a. CONTRACT NUMBER
In-house

5b. GRANT NUMBER

5c. PROGRAM ELEMENT NUMBER
62102F

6. AUTHOR(S)
Randall S. Hay and Michael K. Cinibulk (AFRL/RXCC)
Emmanuel E. Boakye, Kristin Keller, Pavel S. Mogilevsky, and T.A. Parthasarathy (UES, Inc.)
M. Ahrens (Wright State University)

5d. PROJECT NUMBER
4347

5e. TASK NUMBER
50

5f. WORK UNIT NUMBER
LN102102

7. PERFORMING ORGANIZATION NAME(S) AND ADDRESS(ES)
Composites Branch (AFRL/RXCC)
Structural Materials Division
Air Force Research Laboratory, Materials and Manufacturing Directorate
Wright-Patterson Air Force Base, OH 45433-7750
Air Force Materiel Command, United States Air Force

8. PERFORMING ORGANIZATION REPORT NUMBER

9. SPONSORING/MONITORING AGENCY NAME(S) AND ADDRESS(ES)
Air Force Research Laboratory
Materials and Manufacturing Directorate
Wright-Patterson Air Force Base, OH 45433-7750
Air Force Materiel Command
United States Air Force

10. SPONSORING/MONITORING AGENCY ACRONYM(S)
AFRL/RXCC

11. SPONSORING/MONITORING AGENCY REPORT NUMBER(S)
AFRL-RX-WP-TP-2012-0376

12. DISTRIBUTION/AVAILABILITY STATEMENT
Approved for public release; distribution unlimited. Preprint to be submitted to 36TH International Conference & Expo Advanced Ceramics.

13. SUPPLEMENTARY NOTES
The U.S. Government is joint author of this work and has the right to use, modify, reproduce, release, perform, display, or disclose the work. PA Case Number and clearance date: 88ABW-2012-0909, 24 February 2012. This document contains color.

14. ABSTRACT
In prior work, the synthesis of α, β and γ-Re2Si2O7 powders (Re= Y and Ho) at temperatures from 1000° to 1400°C h in air was reported, along with the Vickers hardness of dense γ-Y2Si2O7 and γ-Ho2Si2O7 polymorphs. Dense γ-Y2Si2O7 and γ-Ho2Si2O7 pellets were made by a pressureless sintering technique at 1400°C/8h. Using the pressureless sintering technique, densification of α and β-Y2Si2O7 powder compacts at their phase formation temperature (1000°C - 1200°C) was not successful and prevented the determination of their hardness values. In this work, the field assisted sintering technique (FAST) was used to form dense α, β and γ-Y2Si2O7 pellets at a pressure of 20KN and temperatures of 1050°C to 1200°C. Subsequently, their Vickers hardness was measured. SCS-0 fibers were also incorporated into α, β and γ-Re2Si2O7 matrices and densified at 1050°C to 1200°C/1 h using the FAST approach. Fiber push-out experiments were conducted, and the average sliding stress values were determined.

15. SUBJECT TERMS
ceramic matrix composite, fiber coating, rare-earth disilicate, oxidation

16. SECURITY CLASSIFICATION OF:			17. LIMITATION OF ABSTRACT:	NUMBER OF PAGES	19a. NAME OF RESPONSIBLE PERSON (Monitor)
a. REPORT	**b. ABSTRACT**	**c. THIS PAGE**	SAR	12	Randall Hay
Unclassified	Unclassified	Unclassified			**19b. TELEPHONE NUMBER** *(Include Area Code)* N/A

Standard Form 298 (Rev. 8-98)
Prescribed by ANSI Std. Z39-18

Processing and Testing $Re_2Si_2O_7$ Matrix Composites

Emmanuel E. Boakye, Kristin Keller, Pavel S. Mogilevsky, T. A. Parthasarathy
Air Force Research Laboratory
UES, Inc., Dayton, OH

Randall S. Hay, Michael K. Cinibulk
Air Force Research Laboratory
Materials and Manufacturing Directorate
WPAFB, OH

M. Ahrens
Wright State University
Fairborn, OH *

Abstract

In prior work, the synthesis of α, β and γ-$Re_2Si_2O_7$ powders (Re= Y and Ho) at temperatures from 1000° to 1400°C h in air was reported, along with the Vickers hardness of dense γ-$Y_2Si_2O_7$ and γ-$Ho_2Si_2O_7$ polymorphs. Dense γ-$Y_2Si_2O_7$ and γ-$Ho_2Si_2O_7$ pellets were made by a pressureless sintering technique at 1400°C/8h. Using the pressureless sintering technique, densification of α and β-$Y_2Si_2O_7$ powder compacts at their phase formation temperature (1000°C - 1200°C) was not successful and prevented the determination of their hardness values. In this work, the field assisted sintering technique (FAST) was used to form dense α, β and γ-$Y_2Si_2O_7$ pellets at a pressure of 20KN and temperatures of 1050°C to 1200°C. Subsequently, their Vickers hardness was measured. SCS-0 fibers were also incorporated into α, β and γ-$Re_2Si_2O_7$ matrices and densified at 1050°C to 1200°C/1 h using the FAST approach. Fiber push-out experiments were conducted, and the average sliding stress values were determined.

1.   Introduction

The application of SiC/SiC ceramic matrix composites (CMCs) is limited by mechanical property degradation in oxidizing environments. Several methods are used to minimize the oxidation of BN or carbon fiber-matrix interphases in SiC/SiC CMCs;[1] however, an ideal solution would be to replace BN or carbon with a material that does not oxidize. The rare-earth disilicates are attractive candidates.[2]

Among the rare earth disilicates, yttrium disilicate ($Y_2Si_2O_7$) is the most thoroughly studied. It has five polymorphs and is refractory, melting at 1775°C.[3-8] Its γ-polymorph (γ-$Y_2Si_2O_7$) is a "quasi-ductile" ceramic[5-6] and has comparable mechanical properties to $LaPO_4$ (monazite), which has been demonstrated to function as a weak fiber-matrix interphase in oxide-oxide CMCs.[6,9-10] Both are soft (Vickers hardness ~6 GPa) and machineable. However, monazite decomposes in the reducing atmospheres typically used for processing SiC-SiC CMCs, and the rare earth disilicate $La_2Si_2O_7$ forms by reaction between SiO_2 and $LaPO_4$ under reducing conditions.[11-13] An alternate oxide coating, therefore, that is stable in reducing environments is needed. In addition to its softness, γ-$Y_2Si_2O_7$ is thermochemically compatible with SiC and SiO_2,[14] and it has a thermal expansion coefficient (~4x10^{-6}°C^{-1}) that is similar to SiC.[15] This combination of properties induced the investigation of $Re_2Si_2O_7$ as a possible fiber-matrix interphase for SiC/SiC CMCs.

The rare-earth disilicates are commonly prepared by a variety of methods, including conventional solid-state reaction of mixed oxides (RE_2O_3 and SiO_2), calcination of rare-earth disilicate sol-gel precursors, and hydrothermal processing.[16-22] In our prior work, the formation of α, β, and γ-$Re_2Si_2O_7$ powders (Re= Y and Ho) at temperatures between 1000° - 1400°C/air was reported. Precursors to $Y_2Si_2O_7$ and $Ho_2Si_2O_7$ were made by adding colloidal silica to solutions of yttrium and holmium nitrate.

LiNO$_3$ was added to decrease the formation temperature of the γ-polymorphs. Dense γ-Y$_2$Si$_2$O$_7$ and γ-Ho$_2$Si$_2$O$_7$ pellets were made by pressureless sintering at 1400°C/8h and hardness measurements were completed using the Vickers indentation method. Densification of α and β-Y$_2$Si$_2$O powder compacts at their phase formation temperatures of 1000°C - 1200°C using pressureless sintering was not successful; therefore, their hardness values were not measured. In this work, dense α, β and γ-Y$_2$Si$_2$O pellets were made using the field assisted sintering technique (FAST) and hardness measurements were completed using the Vickers indentation method. Further, SCS-0 fibers were incorporated into α, β, γ-Re$_2$Si$_2$O$_7$ matrices and densified at 1050-1200°C/1 h using the FAST approach. Fiber push-out experiments were conducted and the measured sliding stress values are reported and discussed.

2.   Experimental

2.1 Precursor Synthesis and Characterization

Precursors to Y$_2$Si$_2$O$_7$ and Ho$_2$Si$_2$O$_7$ were made by adding colloidal silica to solutions of yttrium and holmium nitrate, as reported previously.[2] For the Y$_2$Si$_2$O$_7$ precursor, 12.7 g of Y(NO$_3$)•6H$_2$O were dissolved in 50 mL of deionized water to make a solution of pH ~1. The sol pH was determined using a pH/ion meter (Corning Inc., Corning NY). Silica (2.0 – 2.8 g) was added in the form of a sol with a pH of 10. For the Ho$_2$Si$_2$O$_7$ precursor, 14.7 g of Ho(NO$_3$)•5H$_2$O were added to 50 mL of deionized water and 2 g of silica was then added. In some cases, 0.12 g of LiNO$_3$ was added to the Y and Ho-derived precursor. The mixtures were dried in an oven for 72 h to form SiO$_2$/Y(OH)$_3$ and SiO$_2$/Ho(OH)$_3$ and then heated at 1050ºC in air. The subsequent powders were characterized by X-ray diffraction (XRD) with Cu-Kα radiation (Model Rotaflex, Rigaku Co., Tokyo, Japan).

2.2 Formation and Densification of Pellets

SiO$_2$/Y(OH)$_3$ and SiO$_2$/Ho(OH)$_3$ dispersions with and without Li dopant were dried and then heat treated at 1050°C/1 h. Heat treated powders without Li formed α-Y$_2$Si$_2$O$_7$ and α-Ho$_2$Si$_2$O$_7$, while heat treated powders doped with Li formed β-Y$_2$Si$_2$O$_7$ and β-Ho$_2$Si$_2$O$_7$. Powders in the α and β phases were ball milled in isopropanol using alumina milling media. Polyvinyl butyral resin (3 vol%) was added as a binder. After milling, the powder samples were characterized by XRD to confirm the retention of the α and β phases. The milled slurry was separated and dried at 120°C for 18 h. The dried powder was uniaxially pressed into pellets and densified by the FAST approach at a pressure of 20KN and at temperatures of 1050°C, 1100°C and 1200°C. The dense pellets were ~20 mm in diameter and ~3 mm in height, with relative densities greater than 90%. Density measurements were gathered using the Archimedes method.

2.3. Indentation and Characterization

The hardnesses of the sintered pellets were measured by Vickers indentation at loads in the range of 50 g to 1000 g using a Buehler (Lake Bluff, IL) Hardness Tester 1600-2007. Indented samples were examined with FEI (Hillsboro, Oregon) scanning electron microscopes (SEM, Models Sirion and Quanta) with an X-ray energy dispersive spectroscopy (EDS) system operating at 5-20 kV. Foils for transmission electron microscopy (TEM, Philips CM200, FEI, Hillsboro, Oregon) were cut from areas below the Vickers indentations using an FEI (Hillsboro, Oregon) Focused Ion Beam (FIB) Dual Beam DB 235 workstation equipped with Omniprobe (Dallas, Texas) AutoProbe™ 200 micromanipulator.

2.4 Fiber Push-Out

SCS-0 fibers were sandwiched between two green pellets and densified at 1050 °C, 1100°C, and 1200°C for 1 h in vacuum using the FAST approach with a force of 20 kN. An approximately 0.4 mm thick cross sectional specimen was prepared for push-out studies; in this case, the fibers ran perpendicular

to the polished surface. A fiber push-out testing apparatus (Process Equipment, Inc., Troy, OH) was used to obtain load displacement curves. The sliding stress was calculated based on a fiber diameter of 140 μm and using the minimum load, which corresponds to the load where fiber sliding stopped.

3. Results and Discussion

3.1 Densification of $Y_2Si_2O_7$ and $Ho_2Si_2O_7$

As reported previously, heat treatment of $SiO_2/Y(OH)_3$ and $SiO_2/Ho(OH)_3$ dispersions without Li at 1050°C formed α-$Y_2Si_2O_7$ and α-$Ho_2Si_2O_7$ powders.[2] Alternately, with Li doping, $SiO_2/Y(OH)_3$ and $SiO_2/Ho(OH)_3$ dispersions heat treated at 1050°C formed β-$Y_2Si_2O_7$ and β-$Ho_2Si_2O_7$. The α and β powders formed at 1050C° were uniaxially pressed into pellets and densified by the FAST process at a pressure of 20KN and at temperatures of 1050°C, 1100°C and 1200°C. Table 1 and Figure 1 summarize the XRD results after densification. X-ray diffraction studies showed that α-$Y_2Si_2O_7$ pellets, densified at 1050°C, retained the α phase, whereas α-$Y_2Si_2O_7$ pellets densified at 1100°C transformed to β-$Y_2Si_2O_7$. In the case of Li-doped β-$Y_2Si_2O_7$ and β-$Ho_2Si_2O_7$ pellets, densification at 1200°C formed γ-$Y_2Si_2O_7$ and γ-$Ho_2Si_2O_7$. (Table 1, Figure 1). The relative densities of the pellets were determined from the measured and the theoretical densities shown in parentheses. The relative densities were calculated as the percentage of the measured to the theoretical density. The α, β and γ dense pellets formed by the FAST approach had relative densities > 90%.

Table 1. Formation of dense $Y_2Si_2O_7$ and $Ho_2Si_2O_7$ pellets using the FAST technique

Starting Powder	FAST Temperature (°C)	Final Phase After FAST	Density Measured (Theoretical)	Relative Density %
α-$Y_2Si_2O_7$	1050	α	3.8 (4.18)	91
α-$Y_2Si_2O_7$	1100	β	3.8 (4.02)	94
β-$Y_2Si_2O_7$ + Li	1200	γ	3.8 (4.04)	94
β-$Ho_2Si_2O_7$+Li	1200	γ	5.8 (6.30)	92

3.2 Hardness

SEM micrographs of α, β, and γ-$Y_2Si_2O_7$ pellets after Vickers indentation are shown in Figure 2. In addition to the pure rare-earth disilicate, SEM/EDS showed silica as a second phase in all cases. SEM/EDS showed silica-rich dark regions with almost no yttrium in the EDS spectrum and a grey region with very similar yttrium and silica intensities.[2] The experimental hardness values were obtained from Vickers indentation and these values represent the sum of the hardnesses of the pure rare earth disilicate and silica. The hardness of pure rare earth-silicate was calculated using the rule of mixtures, assuming that the hardness of pure silica is 1GPa. Results of the experimental measurements and the theoretical determined hardness values for dense α, β, γ-$Y_2Si_2O_7$ and γ-$Ho_2Si_2O_7$ pellets are summarized in Table 2. The measured Vickers hardness values were very similar for α, β, γ-$Y_2Si_2O_7$ and γ-$Ho_2Si_2O_7$ (~7GPa) and were consistent with our previous reported γ-$Y_2Si_2O_7$ hardness value of ~ 6GPa for samples densified using a pressureless sintering technique at 1400°C/8h.
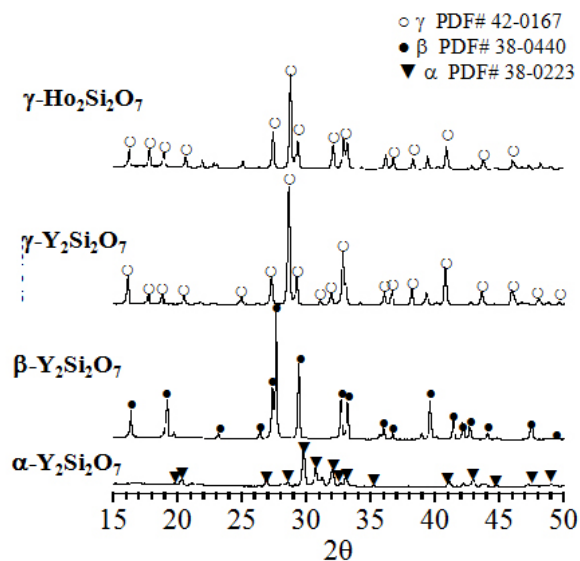
Figure 1. X-ray powder diffraction patterns of densified α, β, γ-Y$_2$Si$_2$O$_7$and γ-Y$_2$Si$_2$O$_7$ densified at 1050°C, 1100°C and 1200°C
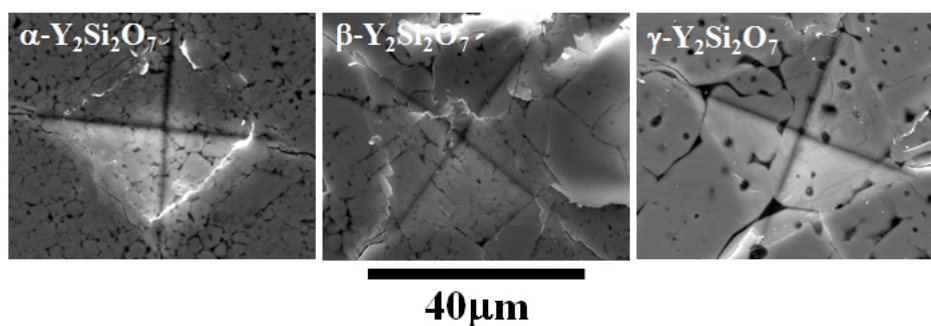
Figure 2. SEM micrographs of α, β, and γ-Y$_2$Si$_2$O$_7$ pellets after Vickers indentation

Table 2. Hardness of α, β, γ-Y$_2$Si$_2$O$_7$ and γ-Y$_2$Si$_2$O$_7$ densified by FAST technique

Final phase after FAST	Experimental Density	Theoretical Density	Silica volume fraction	Re- silicate volume fraction	Experimental Hardness (GPa)	Calculated Hardness (GPa)
α-Y$_2$Si$_2$O$_7$	3.8	4.18	0.19	0.81	6.7	8.1
β-Y$_2$Si$_2$O$_7$	3.8	4.02	0.12	0.88	6.6	7.4
γ-Y$_2$Si$_2$O$_7$ + Li	3.8	4.04	0.13	0.87	7.0	7.9
γ-Ho$_2$Si$_2$O$_7$ +Li	5.8	6.30	0.12	0.88	5.9	6.6

3.3 Deformation Behavior under Indentation

As mentioned previously, the mechanical properties of γ-$Y_2Si_2O_7$ are comparable to monazite, which is soft and deforms plastically by multiple dislocation glide and twinning systems.[23-25] To study deformation mechanisms that may operate in α, β and γ-$Y_2Si_2O_7$, TEM foils were machined beneath indented regions of sintered $Y_2Si_2O_7$ using FIB. A cross-sectional TEM image of an indent made on sintered γ-$Y_2Si_2O_7$ is shown in Figure 3. It shows extensive fracture and plastic deformation. ***Preliminary studies of the α and β-$Y_2Si_2O_7$ polymorphs also indicated extensive deformation (Figure 4).*** More detailed studies of these features are in progress.
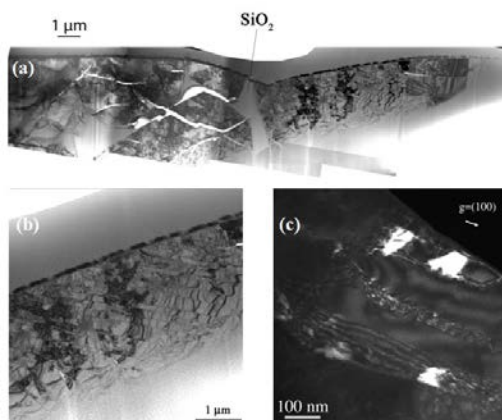
Figure 3. Plastic deformation under an indent made on sintered γ-$Y_2Si_2O_7$ (cross-sectional TEM image): (a) overview, bright field; (b) multiple slip bands/active dislocation glide, bright field; (c) $(11\bar{1})$ staking faults, dark field
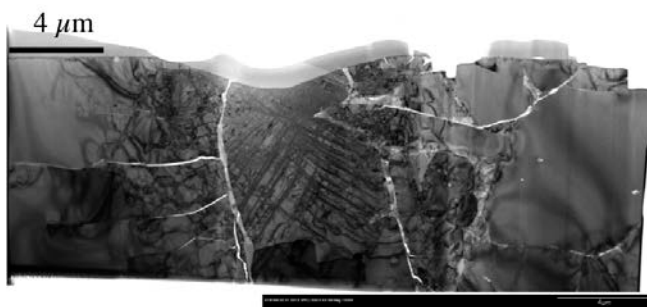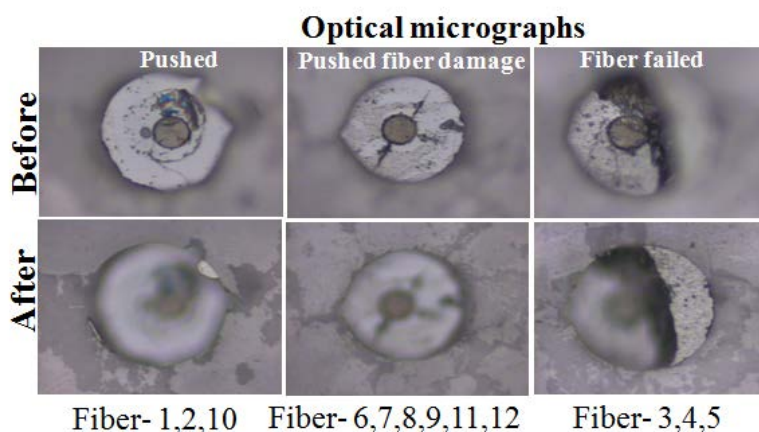

Figure 4. Extensive deformation in α-$Y_2Si_2O_7$

3.4 Fiber Push-Out

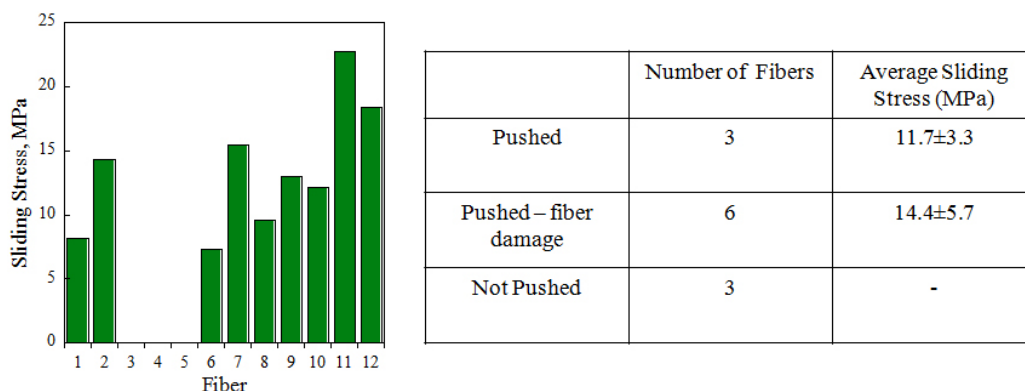Previous results showed that SCS-0 fibers in dense γ-$Ho_2Si_2O_7$ and γ-$Y_2Si_2O_7$ matrices debond and push-out with sliding stresses of 30-60 MPa,[26-27] within the range reported for C, BN, and $LaPO_4$ coatings. Similar to the observation made for $LaPO_4$/alumina composites, SEM showed smearing of the γ-$Y_2Si_2O_7$ matrix. Furthermore, as with the plastic deformation observed for the $LaPO_4$/alumina interface, TEM observation was consistent with intense deformation at the SCS-0 fiber/matrix interface. These results indicate that the γ-$Y_2Si_2O_7$ may function as a weak interface for toughening SiC/SiC composites. However, the γ-$Y_2Si_2O_7$ matrix forms at relatively high temperatures (> 1400°C) and may

cause fiber damage during the coating processing. The α and β polymorphs form at relatively lower temperatures (<1200°C) and may therefore retain the fiber strength. The fact that the α and β polymorphs have similar hardnesses as the γ polymorph implies that the α and β-$Y_2Si_2O_7$ may work as well. Pushout measurements were done for SCS fibers in α and β-$Y_2Si_2O_7$ matrices to measure the interface sliding stress. SCS-0 fibers were sandwiched between two green α-$Y_2Si_2O_7$ pellets and densified at 1050 °C and 1100°C for 1 h using the FAST approach. For the SCS-0/α-$Y_2Si_2O_7$ composite densified at 1050°C, the $Y_2Si_2O_7$ matrix retained the α phase. Alternately, the α-$Y_2Si_2O_7$ matrix transformed to β-$Y_2Si_2O_7$ in composites densified at 1100°C.

Fiber push-out results for SCS fibers in the β-$Y_2Si_2O_7$ matrix are summarized in Figures 5 and 6. The push-out data is classified into 3 groups according to the extent of defocus of the optical micrographs after the fiber push-out. These groups consist of: a) pushed, b) pushed but with fiber damage and c) not pushed. The average sliding stress is plotted and tabulated in Figure 6. Fibers that pushed with damage (b) showed similar average sliding stresses to fibers that pushed (a). The average sliding stress was 11.7± 3.3 GPa and 14.4±5.7 for fibers that pushed and pushed with damage, respectively. SEM investigation of fibers that pushed with damage showed push-out in the front and back-end of the pushed out specimen, confirming fiber sliding after push-out.

Figure 5. Optical micrographs of pushed SCS-0 fibers in the β-$Y_2Si_2O_7$ matrix

	Number of Fibers	Average Sliding Stress (MPa)
Pushed	3	11.7±3.3
Pushed – fiber damage	6	14.4±5.7
Not Pushed	3	-

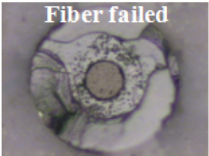**Figure 6.** Sliding stress of SCS fibers pushed-out in the β-$Y_2Si_2O_7$ matrix

The data for the pushed out fiber in the α-$Y_2Si_2O_7$ matrix was very erratic and was classified into pushed and unpushed sets (Figure 7). The average sliding stress was 28.0±3.8. For fibers that pushed, SEM analysis showed fiber sliding in the front end, but the back-end showed very little or no sliding (Figure 8). In the worst case scenario, the matrix was observed to be pushing with the fiber, which indicates strong fiber/matrix bonding. CTE measurements of the α, β, and γ polymorphs of $Y_2Si_2O_7$ and $Ho_2Si_2O_7$ show a CTE of ~ 8 for the α phase.[28] The β and γ phases have a similar CTE of ~4.[28] The composites were formed at 1050°C-1200°C. During cooling, the α-$Y_2Si_2O_7$, with a higher CTE, contracts to a greater extent and exerts a radial compressive stress on the fiber, which makes it more difficult to push. The compressive stresses will increase along the fiber length, thus making it more difficult for the fibers to push in the back ends.
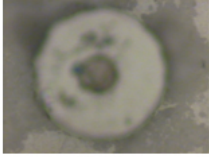

	Number of Fibers	Average sliding stress (MPa)
Pushed	3	28.0±3.8
Pushed – fiber damage	2	-
Not Pushed	5	-
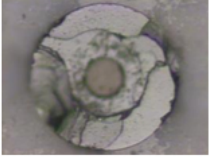
Figure 7. Push-out data for SCS-0 fibers in α-$Y_2Si_2O_7$ matrix
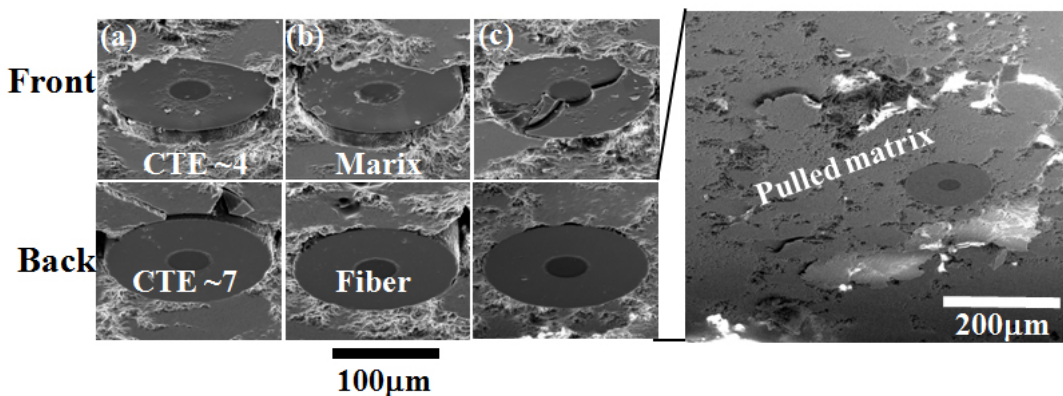
Figure 8. Scanning electron micrographs of pushed SCS-0 fibers in an α-$Y_2Si_2O_7$ matrix

4. Summary and Conclusions

Dense α, β and γ-$Y_2Si_2O_7$ pellets were formed using the FAST technique at a pressure of 20KN and temperatures of 1050°C to 1200°C. Vickers hardness values for α, β, and γ-$Y_2Si_2O_7$ polymorphs were similar (~7GPa). TEM analysis of samples directly beneath the indentations suggested that both extensive dislocation slip and fracture were active. Preliminary results showed that SCS-0 fibers in dense β, γ-$Y_2Si_2O_7$ matrices debonded and pushed-out with sliding stresses of 15-60 MPa, within the range reported for C, BN, and LaPO$_4$ coatings. Fibers in the α-$Y_2Si_2O_7$ matrix showed poor and erratic pushout

behavior due to the radial compressive stresses that developed on the fibers as result of the differences in CTEs (fiber ~4 and matrix ~8).

References

1   Kerans, R. J., Hay, R. S., Parthasarathy, T. A. & Cinibulk, M. K. Interface Design for Oxidation Resistant Ceramic Composites. *J. Am. Ceram. Soc.* **85**, 2599-2632 (2002).

2   Boakye, E. E., Mogilevsky, P., Hay, R. S. & Cinibulk, M. K. Rare-Earth Disilicates as Oxidation-Resistant Fiber Coatings for Silicon Carbide Ceramic Matrix Composites. *J Am. Ceram. Soc.* **94**, 1716-1724 (2011).

3   Escudero, A., Alba, M. D. & Becerro, A. I. Polymorphism in the Sc2Si2O7-Y2Si2O7 System. *J. Solid State Chem.* **180**, 1436-1445 (2007).

4   Escudero, A. & Beccerro, A. I. Stability of Low Temperature Polymorphs (y and a) of Lu-doped $Y_2Si_2O_7$. *J. Phys. Chem. Solids* **68**, 1348-1353 (2007).

5   Sun, Z., Zhou, Y. & Li, M. Low Temperature Synthesis and Sintering of g-Y2Si2O7. *J. Mat. Sci.* **21**, 1443-1450 (2006).

6   Sun, Z., Zhou, Y., Wang, J. & Li, M. g-Y2Si2O7, a Machinable Silicate Ceramic: Mechanical Properties and Machinability. *J. Am. Ceram. Soc.* **90**, 2535-2541 (2007).

7   Felsche, J. Polymorphism and Crystal data on the Rare-Earth Disilicates of the Type Re2Si2O7. *J. Less-Common Metals* **21**, 1-14 (1970).

8   Seifert, H. J. *et al.* Yttrium Silicate Coatings on Chemical Vapor Deposition-SiC-Precoated C/C-SiC: Thermodynamic Assessment and High-Temperature Investigation. *J. Am. Ceram. Soc.* **88**, 424-430 (2005).

9   Wang, J. Y., Zhou, Y. C. & Lin, Z. J. Mechanical Properties and Atomistic Deformation Mechanism of g-Y2Si2O7 from First-Principles Investigations. *Acta mat.* **55**, 6019-6026 (2007).

10   Keller, K. A. *et al.* Effectiveness of Monazite Coatings in Oxide/Oxide Composites After Long Term Exposure at High Temperature. *J. Am. Ceram. Soc.* **86**, 325-332 (2003).

11   Boakye, E. E. *et al.* Monazite Coatings on SiC Fibers I: Fiber Strength and Thermal Stability. *J. Am. Ceram. Soc.* **89**, 3475-3480 (2006).

12   Mogilevsky, P., Boakye, E. E., Hay, R. S., Welter, J. & Kerans, R. J. Monazite Coatings on SiC Fiber Tows II: Oxidation Protection. *J. Am. Ceram. Soc.* **89**, 3481-3490 (2006).

13   Cinibulk, M. K., Fair, G. E. & Kerans, R. J. High-Temperature Stability of Lanthanum Orthophosphate (Monazite) on Silicon Carbide at Low Oxygen Partial Pressure. *Am. Ceram. Soc.* **91**, 2290–2297 (2008).

14   Cupid, D. M. & Seifert, H. J. Thermodynamic Calculations and Phase Stabilities in the Y-Si-C-O System. *J. Phase Equil. Diff.* **28**, 90-100 (2007).

15   Sun, Z., Zhou, Y., Wang, J. & Li, M. Thermal Properties and Thermal Shock Resistance of g-$Y_2Si_2O_7$. *J. Am. Ceram. Soc.* **91**, 2623-2629 (2008).

16   Becerro, A. I., Naranjo, M., Perdigon, A. C. & Trillo, J. M. Hydrothermal Chemistry of Silicates: Low Temperature Synthesis of y-Yttrium Disilicate. *J. Am. Ceram. Soc.* **86**, 1592-1594 (2003).

17   Ranganathan, V. & Klein, L. C. Sol-gel Synthesis of Erbium-doped Yttrium Silicate Glass-ceramics. *J. Non-Cryst. Solids* **354**, 3567-3571 (2008).

18   Zhou, P., Yu, X., Yang, S. & Gao, W. Synthesis of $Y_2Si_2O_7$:Eu Nanocrystal and its Optical Properties. *J. Lumin.* **124**, 241-244 (2007).

19   Diaz, M. G.-C. I., Mello-Castanho, S., Moya, J. S. & Rodriguez, M. A. Synthesis of Nanocrystalline Yttrium Dislicate Powder by Sol-Gel Method. *J. Non. Cryst. Sol.* **289**, 151-154 (2001).

20   Diaz, M. Synthesis, Thermal Evolution, and Luminescence Properties of Yttrium Disilicate Host Matrix. *Chem. Mater.* **17**, 1774-1782 (2005).

21   Maier, N., Rixecker, G. & Nickel, K. G. Formation and Stability of Gd, Y, Yb and Lu Disilicates and their Solid Solutions. *J. Solid State Chem.* **179**, 1630-1635 (2006).

22   Parmentier, J. Phase Transformations in Gel-Derived and Mixed-Powder-Derived Yttrium Disilicate, $Y_2Si_2O_7$, by X-Ray Diffraction and ^{29}Si MAS NMR. *J. Solid State Chem.* **149**, 16-20 (2000).

23   Hay, R. S. Monazite and Scheelite Deformation Mechanisms. *Ceram. Eng. Sci. Proc.* **21**, 203-218 (2000).

24   Hay, R. S. (120) and (12$\underline{2}$) Monazite Deformation Twins. *Acta mater.* **51**, 5255-5262 (2003).

25   Hay, R. S. Climb-Dissociated Dislocations in Monazite. *J. Am. Ceram. Soc.* **87**, 1149-1152 (2004).

26   Rebillat, F. *et al.* Interfacial Bond Strength in SiC/C/SiC Composite Materials, as Studied by Single-Fiber Push-Out Tests. *J. Am. Ceram. Soc.* **81**, 965-978 (1998).

27   Morgan, P. E. D. & Marshall, D. B. Ceramic Composites of Monazite and Alumina. *J. Am. Ceram. Soc.* **78**, 1553-1563 (1995).

28   T. Key, Presley, K., Boakye, E. E. & Hay, R. S. in *36th International Conference and Exposition on Advanced Ceramics and Composites.*